Experiments in Fluids 21 (1996) 201-208 © Springer-Verlag 1996

Suggestive correctional methods for PIV image biasing caused by a rotating mirror system

S. D. Lee, S. H. Chung, K. D. Kihm

Abstract A rotating mirror is widely used to generate the velocity shift that can resolve the directional ambiguities of PIV (particle image velocimetry) measurements. The rotating mirror system inevitably creates the normal displacement of the resulting PIV images and causes systematic image errors. Two corrective methods are proposed to eliminate or reduce the image biasing in PIV system. The use of two linearly traversing mirrors, instead of a single rotating mirror, shows that image biasing can be eliminated and the velocity shift well generated. As a second option, two co-rotating mirrors, instead of one, can reduce the image biasing with a maximum velocity shift available. Detailed imaging kinematics of the two suggestive methods are presented to lead to designing of practical devices that improve the PIV capabilities by reducing the systematic image errors.

1 Introduction

The PIV data analysis needs to resolve the flow directional ambiguities by determining the sign of the particle displacement between the two superimposed recordings. One wellaccepted method to resolve these ambiguities is a crosscorrelation between recorded images (Keane and Adrian 1992). Merzkirch et al. (1994) show a successful application of the cross-correlation method to measure a natural convective flow. The cross-correlation method works primarily for relatively low velocity flows recorded with multiple video PIV systems since the video framing rate limits the maximum velocity to be measured. The most widely used method for discriminating the particle displacement direction is to artificially generate a velocity shift of the second recorded image using a rotating mirror (Adrian 1986). The shift velocity is added to the flow field so that all the apparent particle displacements are consistent in their sign and the directional ambiguities are resolved. Subtracting the shift velocity from the measured particle image velocity determines the real flow velocity.

The rotating mirror system generates an intrinsic problem of aberrations in the imaging of the particles. When the mirror is rotated, the reflected image, which also rotates, tilts and shifts simultaneously between the two exposures in PIV. The image tilting generates nonzero normal velocity component, or equivalently, nonzero normal displacement with respect to the focal plane of the recording system. This induced normal velocity component tilts the perspective view of the particle images and the recorded particle displacement is biased either shorter or longer than it should be. Therefore, the velocity measurement from analyzing the particle displacement recorded with a rotating mirror PIV system is subjected to systematic errors (Oschwald et al. 1995). In addition, the normal displacement of the reflected images from the mirror rotation will make the recorded images blur and the blurred particle images degrade the accuracy of the displacement measurement.

One can extend the PIV capability into three-dimensional measurements by modifying the PIV system to identify and analyze this normal velocity component. Prasad and Adrian (1993) developed a twin-camera stereoscopic system to detect the normal velocity component and to extend the PIV to three-dimensional vector detection.

For widely accepted two-dimensional PIV systems, however, the systematic errors and image blurring problems remain to be addressed. Raffel and Kompenhans (1995) suggested a computational technique to correct the systematic errors as a post-data correction of images already taken by a rotating mirror PIV system. They demonstrated a successful application of the PIV system with enhanced accuracy in detecting the particle image displacement. Though the computational correction technique was able to effectively eliminate the systematic image errors, the image blur problem intrinsically occurring from the normal displacement of the rotating mirror is yet to be resolved.

Two proposed correctional methods that eliminate or reduce the systematic errors and image blurs will use two traversing mirrors or two co-rotating mirrors instead of a single rotating mirror. The key idea is to devise a velocity shifting configuration that does not generate the normal velocity component with respect to the focal plane of the recording system. First,

Received: 8 September 1995/Accepted: 12 March 1996

S. D. Lee, S. H. Chung Department of Mechanical Engineering Seoul National University Seoul 151-742, Korea

K. D. Kihm Department of Mechanical Engineering Texas A&M University College Station, TX 77843-3123, USA

The authors like to acknowledge the partial financial support provided from the Turbo and Power Machinery Research Center (TPMRC) of Seoul National University, Seoul, Korea.

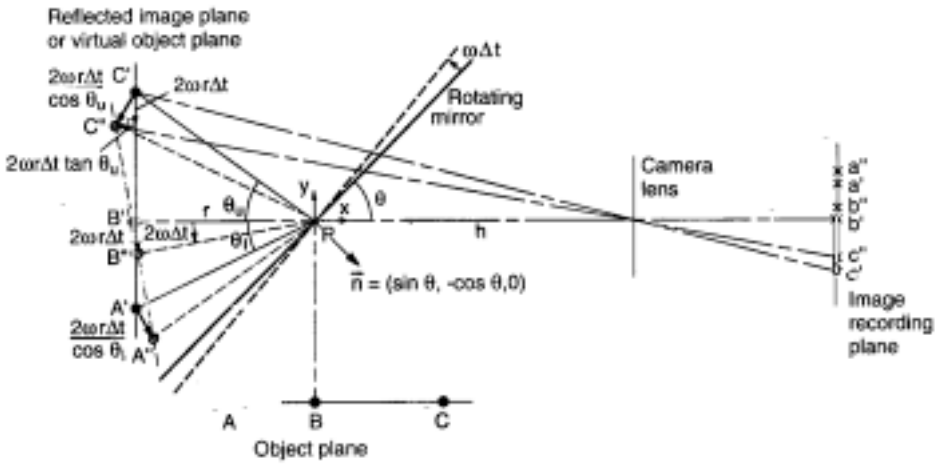

Fig. 1. Illustration of systematic PIV image biasing by a normal displacement concept

the image biasing generated by a rotating mirror method is identified both for a nonzero normal displacement and for a nonzero normal velocity component. The generalized kinematics of mirror imaging is briefly outlined and then the two suggested methods are successively described using the image kinematics.

2

Systematic PIV image biasing generated by a rotating mirror

Generation of the systematic PIV image errors is briefly described using two different approaches: (1) Sect. 2.1 uses a nonzero normal displacement concept induced by the mirror rotation and contributes to the image biasing, and (2) Sect. 2.2 uses a nonzero normal velocity component that biases the PIV image. The former, which Oschwald et al. (1995) also adopted for their description of the image errors, requires a complicated geometrical analysis, whereas the latter more comprehensively explains the image biasing with a simple analysis.

2.1

Explanation by the normal displacement concept

Figure 1 illustrates the systematic errors on images generated by a rotating mirror reflection. A plane mirror, rotating at an angular speed of ω, reflects the three stationary particles, A, B, and C on the object plane. For simplicity, but without losing the general feature, particle B is assumed to be on the optical axis of the system. The image recording plane sees these three particles as if they exist at the virtual locations of A', B', and C' behind the mirror and constructs images a', b', and c'. During the superimposed recording interval Δt in PIV, the virtual objects, A', B', and C' rotate at an angular speed of 2ω with respect to the mirror axis P and move to new virtual object locations A", B", and C". The relative displacement of each pair of the two sets of virtual objects, one at t and the other at t+ Δ t, always carries not only a tangential shift but also a normal component about the image recording plane. The arrows attached to A', B', and C' denote the relative displacements and the expressions next to them represent the magnitudes of the displacement.

This nonzero displacement in the normal direction alters the relative distance between particles on the image recording plane. The approaching normal displacement (A' to A") makes the distance between images slightly larger than it should be without any normal displacement, i.e., $a''b'' > a'b'$ This is because of the tilting of the perspective view of reflected images. When the normal displacement is directed away from the image plane (C' to C"), the distance is slightly reduced, i.e., $c''b'' > c'b'$. Note that the amount of normal displacement,[1] $2\omega r\Delta t \tan \underline{\theta_u}$ or $2\omega r\Delta t \tan \theta_l$ is radially increasing with increasing angle θ measured from the optical axis, whereas the tangential displacement, 2ωrΔ t, is uniformly and uniquely determined by the mirror rotation speed. The normal displacement component will never disappear completely since neither θ_u nor θ_l can be exactly zero when taking two PIV recordings with a rotating mirror configuration. However, the particle located near the optical axis can assume to have a negligibly small displacement in the normal direction due to its extremely small θu and θ_l .

2.2

Explanation by the normal velocity component

Direct consideration of the normal velocity component of a reflected image can better describe the PIV image biasing. Figure 2 schematically shows the reflected image plane of a stationary object and the virtual object located at (x, z) on the reflected image plane. The view point of the camera recording plane sees the reflected image as a virtual object behind the mirror revolving at ω around the rotation axis. L_1 is the object distance measured from the view point of the recording plane and L_2 denotes the distance between the rotating mirror and the object. At an arbitrary image point (x, z), the rotating mirror motion in the counter clockwise direction viewed from the top (Fig. 2) imposes a normal velocity component, $v_n = -2\omega x$, which is symmetrical with respect to the z-axis, and a spatially uniform tangential velocity component, $v_t = 2\omega L_2$. The image biasing occurs from an enlarged or reduced

[1] The exact expression for the normal displacement is derived as $(r/\cos B_u)[\cos(\theta_u-2\omega\Delta t)-\cos\theta_u]$ from the geometrical consideration of the rotating mirror reflection mechanism shown in Fig. 1. This expression can be expanded by Taylor series expansion and the very first term in the series approximates the normal displacement as $2\omega r\Delta t \tan\theta_u$ when $\omega\Delta t$ is sufficiently small.

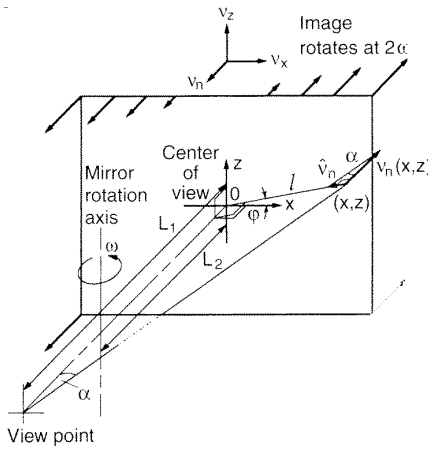

Fig. 2. Illustration of systematic PIV image biasing by a normal velocity component

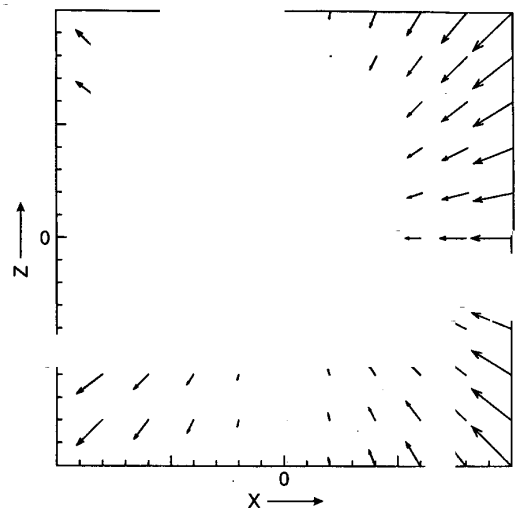

Fig. 3. Spatial distribution of systematic PIV image biasing shown in Eq. (la)

perspective view size when the normal velocity component is non-zero.

Thus, the image biasing is dictated by the magnitude of a tangential projection of the normal velocity component V_n, and for the counter clock rotation as shown in Fig. 2, V_n is given from the trigonometry:

$$\hat{v}_n(x,z) = v_n \tan\alpha = -2\omega x \frac{}{L} = -\frac{2\omega}{L_1} x\sqrt{x^2+z^2} \qquad (1)$$

where a denotes the perspective viewing angle as illustrated in Fig. 2. The normal velocity directing away from the reflected image in the positive $\nearrow$ reduces the perspective view and the normal velocity approaching the image plane in the negative $\nearrow$ enlarges the perspective view.

Figure 3 shows the spatially dependent image biasing per unit time, $\bar{V}_{bias}$(x, z), which is derived from Eq. (1) as

$$\bar{v}_{\text{bias}}(x,y) = (\hat{v}_n \cos\varphi, \hat{v}_n \sin\varphi) = -2\omega x \frac{l}{L_1}\left(\frac{x}{L}, \frac{z}{L}\right)$$
$$= \frac{2\omega}{L_1}(-x^2, -xz) \qquad (1a)$$

The arrow length represents the magnitude of image biasing. The radially inward arrows denote a reduction in the recorded image size, and the radially outward arrows represent an enlargement of the recorded image size. The arrow direction is reversed symmetrically with respect to the z-axis. The magnitudes of the normal displacements are symmetrically distributed along the x-axis. The amount of the actual image biasing in the PIV recording is determined from Eq. (l a) multiplied by the PIV sample period required for the double recordings. The optimal PIV recording period is determined from an combinatorial consideration of the flow speed and the particle image sizes.

It is shown that a rotating mirror inevitably creates the normal displacement because of nonzero normal velocity component. This nonzero normal displacement or velocity component causes the systematic errors of the recorded PIV images.

3 Kinematics of mirror images

A general expression for the reflected image velocity is derived from considering and expanding the basic principle of mirror image kinematics. The derived mathematical expression of the reflected image velocity will describe the two new methods presented in Sects. 4 and 5.

Geometrical considerations of mirror reflection of an arbitrary vector $\boldsymbol{r}$ to a virtual object vector $\boldsymbol{r}'$ gives a simple mathematical expression as (Fig. 4a):

$$\boldsymbol{r}' = \boldsymbol{r} - 2(\boldsymbol{r}\cdot\boldsymbol{n})\boldsymbol{n} = (\delta_{ij} - 2n_i n_j) r_j = R_{ij} r_j = [R]\cdot\boldsymbol{r} \qquad (2)$$

where $[R] \equiv R_{ij} \equiv \delta_{ij} - n_i n_j$ conforms to a reflection matrix and n denotes a unit vector defined normally outward from the mirror surface.

Using the same coordinate configuration shown in Fig. 1, the general expression for the three-dimensional reflection matrix has been derived. When a mirror is rotating around the z-axis (plane rotation with a single degree of freedom) or linearly traversing in the x - y plane, the unit normal vector is given as n = (sin θ, -cos θ, 0) where the mirror angle θ is measured from the x-axis. From Eq. (2), the reflection matrix is expressed as

$$[R] = \delta \quad 2n_i n_j = \begin{vmatrix} 1 & 0 & 0 \\ 0 & 1 & 0 \\ 0 & 0 & 1 \end{vmatrix}$$
$$-2\begin{vmatrix} \sin^2\theta & -\sin\theta\cos\theta & 0 \\ -\sin\theta\cos\theta & \cos^2\theta & 0 \\ 0 & 0 & 0 \end{vmatrix}$$
$$= \begin{vmatrix} \cos 2\theta & -\sin 2\theta & 0 & 0 & 0 \\ \sin 2\theta & \cos 2\theta & 0 & 0 & -1 & 0 \\ 0 & 0 & 1 & 0 & 0 & 1 \end{vmatrix} \qquad (3a)$$

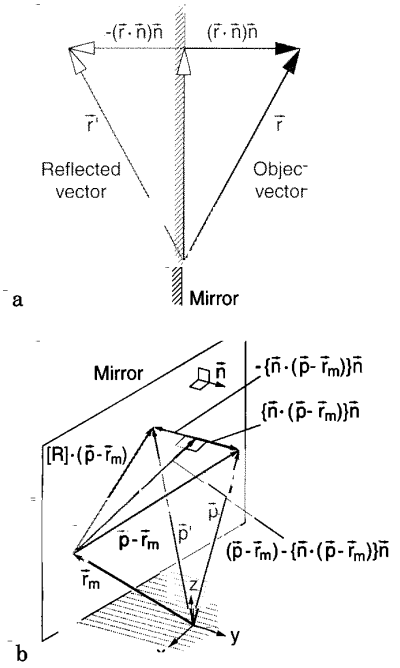

Fig. 4a, b. Mirror image reflections illustrated by ray optics

and its time derivative is

$$\frac{d[R]}{dt} = 2\frac{d\theta}{dt}\begin{bmatrix} -\sin 2\theta & \cos 2\theta & 0 \\ \cos 2\theta & \sin 2\theta & 0 \\ 0 & 0 & 0 \end{bmatrix} = 2\omega\begin{bmatrix} \cos(2\theta+90^\circ) & \sin(2\theta+90^\circ) & 0 \\ \sin(2\theta+90^\circ) & -\cos(2\theta+90^\circ) & 0 \\ 0 & 0 & 0 \end{bmatrix} \quad (3b)$$

Equation (3a) interprets the reflection matrix to form two elementary movements represented by the two matrices: a mirror imaging with respect to the x-z plane and a rotation by an angle 2θ.

The above basic image kinematics is extended to derive a general expression for the reflected image velocity. When an arbitrarily specified position vector $\boldsymbol{r}_m$ specifies the mirror location (Fig. 4b), an expression for the reflection of an arbitrary position vector $\boldsymbol{p}$ to a virtual object vector $\boldsymbol{p}'$ is derived from an extension of Eq. (2):

$$\boldsymbol{p}' = [R] \cdot (\boldsymbol{p} - \boldsymbol{r}_m) + \boldsymbol{r}_m \quad (4)$$

The virtual object or vector is called a reflected image or a reflected vector, respectively, without being confusing with the true image or vector that is ultimately recorded in PIV. A time derivative of the reflected vector $\boldsymbol{p}'$ determines the velocity of the reflected image, i.e.,

$$\boldsymbol{v}_{\text{image}} = \frac{d\boldsymbol{p}'}{dt} = \frac{d}{dt}\{[R] \cdot (\boldsymbol{p} - \boldsymbol{r}_m) + \boldsymbol{r}_m\} \quad (5)$$

Expanding the derivative, applying vector identities, and using useful vector relationships of $d\mathbf{n}/dt = \omega \times \mathbf{n}$ and $\omega = \mathbf{n} \times d\mathbf{n}/dt$ (arithmetic details are presented in Appendix A), Eq. (5) derives a general three-dimensional expression for the reflected image velocity as

$$\boldsymbol{v}_{\text{image}} = 2\boldsymbol{\omega} \times \{[R] \cdot (\boldsymbol{p} - \boldsymbol{r}_m)\} + 2(\boldsymbol{v}_m \cdot \boldsymbol{n})\boldsymbol{n} + [R] \cdot \boldsymbol{v} \quad (6)$$

where ω is the angular velocity of a rotating mirror, v_m denotes the traversing velocity of the mirror defined as $v_m \equiv d\mathbf{r}_m / dt$, and **v** represents the object velocity defined as $v \equiv d\mathbf{p} / dt$. Note that the mirror rotation vector ω has only the z-directional component for the plain mirror rotation and the first term on the RHS, due to the vector product by ω, will not carry any z-directional component. This first term on the RHS of Eq. (6) represents the portion of the image velocity created by the plain mirror rotation and this portion of the image velocity exists only in the x -y plane. The second term is a contribution from the mirror traverse perpendicular to the mirror surface. When the mirror traverse takes place in the plane perpendicular to the mirror surface, this term also retains its component within the x - y plane. The third term reflects the mirror imaging of the real velocity of a moving object, v. The object velocity can be arbitrarily three-dimensional and so be the third term. In fact, the general expression for the image velocity $\mathbf{v}_{\text{image}}$ in Eq. (6) can be three-dimensional only if the third term, the object velocity, is three-dimensional.

The first term in Eq. (6) can be subjected to be time dependent as the particle position vector p changes with the particle movement and/or the reflection matrix [R] alters in time for the special case of θ = θ (t). The second and third terms remain time invariant as long as the mirror traverses at a constant velocity v_m and the particle velocity remains steady at v during the PIV sample period. However, as will be shown in Sects. 4 and 5, the recorded PIV image velocity $\mathbf{v}_{\text{image}}$ is invariant with respect to time when the mirrors are under plain motion on the x -y plane or the mirrors are rotating with a single degree of freedom, i.e., around one rotating axis.

4 Double reflection by two traversing mirrors

As discussed in Sect. 2, the image biasing comes from a nonzero normal displacement which is created by the image tilting due to the rotating mirror. The idea is that the proper usage of two traversing but nonrotating mirrors can zero the normal velocity component of the recorded image. The proposed system can eliminate the image biasing and effectively provide the velocity shifting required to resolve the directional ambiguities in PIV measurements.

Figure 5 illustrates a double reflection of a stationary object by two plane mirrors traversing normally at speeds of v, and vZ. For simplicity, the object is assumed to orient vertically with the two mirrors inclined at θ_1, and θ_2, respectively. Since the reflected image rotates from the object by twice the mirror inclination angle (Eq. (3a)), the inclination angle of the first reflected image with respect to the x-axis in Fig. 5 is $2\theta_1 - 90°$. The second reflected image sees the first reflected image as a virtual object and the inclination angle of the second reflected image is expressed as $2\theta_2 - (2\theta_1 - 90°) = 2(\theta_2 - \theta_1) + 90°$.

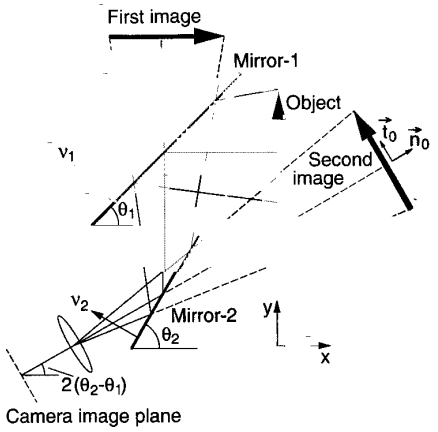

Fig. 5. Schematic of double reflection of an object via two traversing mirrors

The mirror traversing velocities are expressed in terms of x and y components as

$$\boldsymbol{v}_1 = v_1(-\sin\theta_1, \cos\theta_1, 0) \tag{7a}$$

$$\boldsymbol{v}_2 = v_2(-\sin\theta_2, \cos\theta_2, 0) \tag{7b}$$

where v_1 and v_2 represent the magnitudes of normally traversing velocities of the two mirrors, respectively. For the first reflected image of the stationary object through a nonrotating, linearly traversing mirror, the first and third terms of Eq. (6) are zero and the resulting image velocity from the second term is given as v_{image}, $= 2\ v_1$. For the second reflected image, however, the third contribution is no longer zero since the second reflected image sees the first reflected image as a virtual object moving at $_{vimage}$. Therefore, the second reflected image velocity is determined from the second and third contributions of Eq. (6):

$$v_{image2} = [R_2]\cdot v_{image1} + 2\ v_2 = 2\ ([R_2]\cdot v_1 + v_2) \tag{8}$$

$$\boldsymbol{v}_{image_2} = 2\{v_1 \sin(2\theta_2-\theta_1) - v_2 \sin\theta_2, \\ -v_1\cos(2\theta_2-\theta_1) + v_2\cos\theta_2, 0\} \tag{9}$$

in which the image velocity for a stationary object retains two-dimensional motion since the pseudo-object velocity ν_{image1} has only two-dimensional components. The absence of mirror rotation eliminates the first term in Eq. (6) and the image velocity ν_{image2} of Eq. (9) is time invariant when ν_1 and ν_2 are constants.

The condition that eliminates the normal velocity component (with respect to the camera image plane) of the second reflected image is determined from that the inner product of the image velocity, Eq. (9), and the unit normal vector perpendicular to the inclination angle of the second reflected image must vanish, i.e.,

$$0 = \boldsymbol{v}_{image_2}\cdot\boldsymbol{n}_0 = 2\{v_1\sin(2\theta_2-\theta_1) - v_2\sin\theta_2\}\cos(2\theta_2-2\theta_1) \\ +2\{-v_1\cos(2\theta_2-\theta_1) + v_2\cos\theta_2\}\sin\{2\theta_2-2\theta_1\} \tag{10}$$

where the unit normal vector is $\nu_0 \equiv [\cos(2\theta_b - 2\theta_1), \sin(2\theta_b - 2\theta_1), 0]$. Equation (10) is satisfied when the mirror traversing velocity ratio is given as

$$\frac{v_2}{v_1} = \frac{\sin\theta_1}{\sin(2\theta_1-\theta_2)} \tag{11}$$

Under the specified condition that vanishes the normal velocity component of the second reflected image and eliminates the image biasing, an expression for the shifting velocity in the tangential direction is derived from substituting Eq. (11) into Eq. (9):

$$\frac{v_{shift}}{v_1} = 2\left[\left\{\sin(2\theta_2-\theta_1) - \frac{\sin\theta_1\sin\theta_2}{\sin(2\theta_1-\theta_2)}\right\}\{-\sin(2\theta_2-2\theta_1)\}\right. \\ \left.+\left\{-\cos(2\theta_2-\theta_1) + \frac{\sin\theta_1\cos\theta_2}{\sin(2\theta_1-\theta_2)}\right\}\cos(2\theta_2-2\theta_1)\right] \\ = 2\left[\frac{\sin\theta_1}{\tan(2\theta_1-\theta_2)} - \cos\theta_1\right] \tag{12}$$

Figure 6 shows the mirror traversing velocity ratio v_2/v_1 zeroing the normal image velocity and the velocity shift normalized by the first mirror traversing velocity v_{shift}/v_1 as functions of θ_2, for a commonly selected $\theta_1 = 45°$, i.e., from Eqs, (11) and (12) with $\theta_1 = 45°$:

$$\frac{v_2}{v_1} = \frac{1}{\sqrt{2}\cos\theta_2} \tag{11a}$$

$$\frac{v_{shift}}{} = \sqrt{2}(\tan\theta_2 - 1) \tag{12a}$$

For $\theta_2 = 45°$, where the two mirrors are aligned parallel and traversing at the same speed, the normal velocity component of the image is eliminated but the velocity shift is zero so that the directional ambiguity in PIV cannot be resolved. As θ_2 deviates further from θ_1 =45°, the magnitude of velocity shift increases and the system can apply for flows containing larger negative velocity components in magnitude. Simultaneously, the field--of-view of the second reflected image is quickly reduced

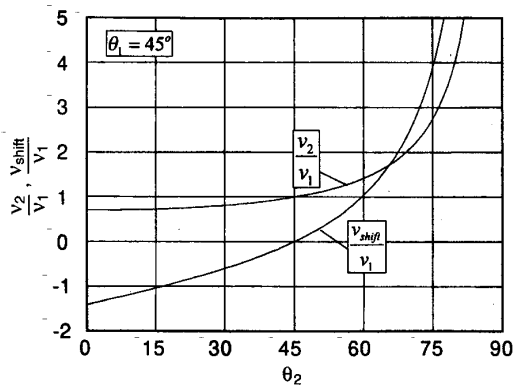

Fig. 6. The mirror traversing velocity ratio v_2/v_1 zeroing the normal image velocity and the dimensionless velocity shift v_{shift}/v_1, as functions of θ_2 for θ_1 =45° for double reflection by two traversing mirrors

because of the image skewing with increasing deviation of the second mirror orientation θ_2 from the first mirror orientation θ_1. Therefore, an optimal combination of θ_1, θ_2, ν_1, ν_2, and ν_{shift}, though these five parameters are not totally independent, must be appropriately determined from the measurement requirements of a specific flow to be tested.

5 Double reflection by two rotating mirrors

Instead of one, a use of two parallel aligned, co-rotating mirrors at the same angular speed can reduce the image biasing when the two PIV images are recorded nearly at the mirror slope angle of 45°. The first reflected image of a stationary object in Fig. 7 rotates counter-clockwise at an angular speed of 2ω around the first mirror axis. Since the first mirror and the image of the first mirror with respect to the second mirror counter-rotate, the rotational motion of the image by the first mirror cancels each other and the second reflected image has only revolutionary displacement with no image tilting. In addition, for the second reflected image recorded at a mirror configuration of a 45° mirror slope angle, the tangential velocity shift is twice the mirror rotational angular speed multiplied by the distance between the first and second mirror axes.

A mathematical description of the co-rotating two-mirror system follows. The general expression for the reflected image velocity, Eq. (6) reduces to a simpler form for a rotating but non-traversing first mirror ($\nu_{m_1} \equiv 0$) with a stationary object ($\nu \equiv 0$):

$$\boldsymbol{v}_{\text{image}_1} = 2\boldsymbol{\omega} \times \{[R] \cdot (\boldsymbol{p} - \boldsymbol{r}_{m_1})\} \tag{13}$$

where r_{m_1} denotes the position vector of the rotational axis of mirror (Fig. 4b) and the subscript '1' denotes the mirror-1 in Fig. 7. When the z axis is set to coincide with the first mirror axis, the mirror position vector r_{m_1} is zero, the mirror rotation vector $\boldsymbol{\omega}$ = (0, 0, ω), and the arbitrary position vector $\boldsymbol{p}$ in

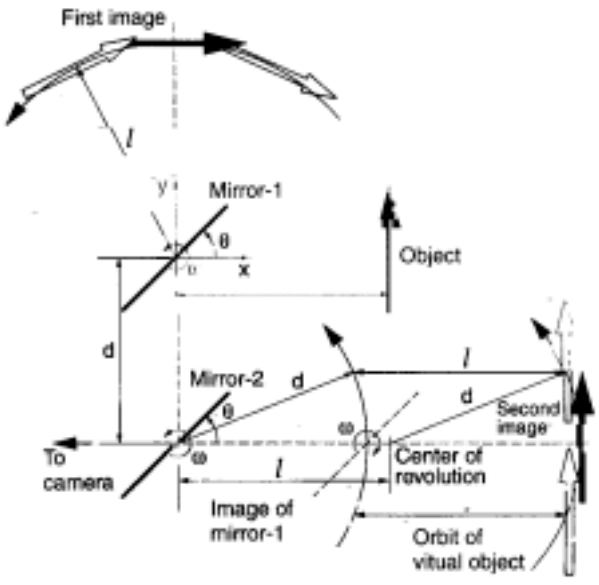

Fig. 7. Schematic of double reflection of an object via two co-rotating mirrors

Fig. 4b can take (x, y, z). Then, the position and velocity of the first reflected image are given respectively as

$$\boldsymbol{p}_{\text{image}_1} = [R] \cdot \boldsymbol{p} = \begin{bmatrix} \cos 2\theta & \sin 2\theta & 0 \\ \sin 2\theta & -\cos 2\theta & 0 \\ 0 & 0 & 1 \end{bmatrix} \begin{pmatrix} x \\ y \\ z \end{pmatrix}$$

$$\boldsymbol{v}_{\text{image}_1} = 2\omega \begin{bmatrix} 0 & -1 & 0 \\ 1 & 0 & 0 \\ 0 & 0 & 0 \end{bmatrix} \times \left(\begin{bmatrix} \cos 2\theta & \sin 2\theta & 0 \\ \sin 2\theta & -\cos 2\theta & 0 \\ 0 & 0 & 1 \end{bmatrix} \begin{pmatrix} x \\ y \\ z \end{pmatrix} \right)$$

$$= 2\omega \begin{bmatrix} 0 & -1 & 0 \\ 1 & 0 & 0 \\ 0 & 0 & 0 \end{bmatrix} \cdot \begin{pmatrix} x\cos 2\theta + y \sin 2\theta \\ x \sin 2\theta - y \cos 2\theta \\ z \end{pmatrix}$$

$$= 2\omega \begin{pmatrix} -x \sin 2\theta + y \cos 2\theta \\ x \cos 2\theta + y \sin 2\theta \\ 0 \end{pmatrix}$$

where θ denotes the mirror slope angle measured with respect to the x-axis as given in Fig. 1 or Fig. 7.

The second mirror position vector can take r_{m2} = (0, -d, 0) where d is the distance between the first and second mirror axes. The second image sees the first image as a virtual object, which traverses at $\mathbf{v}_{\text{image}}$, and Eq. (6) for the second reflected image is expressed as

$$\begin{aligned} \boldsymbol{v}_{\text{image}_2} &= \boldsymbol{\omega} \times \{[R] \cdot (\boldsymbol{p}_{\text{image}_1} - \boldsymbol{r}_{m_2})\} + [R] \cdot \boldsymbol{v}_{\text{image}_1} \\ &= 2\boldsymbol{\omega} \times ([R] : [R] \cdot \boldsymbol{p}) - 2\boldsymbol{\omega} \times ([R] \cdot \boldsymbol{r}_{m_2}) + [R] \cdot \boldsymbol{v}_{\text{image}_1} \end{aligned} \tag{15}$$

Substituting Eqs. (14a) and (14b) into Eq. (15) gives a strikingly simple expression for the second reflected image velocity (the detailed derivation is presented in Appendix B):

$$\boldsymbol{v}_{\text{image}_2} = 2\omega \mathrm{d}(\cos 2\theta, \sin 2\theta, 0) \tag{16}$$

The non-zero x-component of $\mathbf{v}_{\text{image}}$ creates the normal velocity of the second reflected image and the y-component provides a velocity shift for PIV. To note is that the ultimate recorded image of Eq. (16) is time-independent even in the presence of the mirror rotations. The time dependence, or equivalently, the position vector variation of the recorded object, (x, y, z) appearing in the first term disappears as a result of the compensation from the third term (Appendix B).

Figure 8 shows the normal velocity component and the velocity shift normalized by 2ωd as functions of θ. It is emphasized that the two co-rotating mirror system generates a spatially uniform distribution of the normal velocity component throughout the image field for a specified mirror slope of θ, while the single rotating mirror generates a spatially dependent normal velocity distribution (Eq. (1)). Furthermore, the normal component disappears at θ = 45°, and the velocity shift maximizes to a value of 2ωd (Fig. 8). If the two PIV images

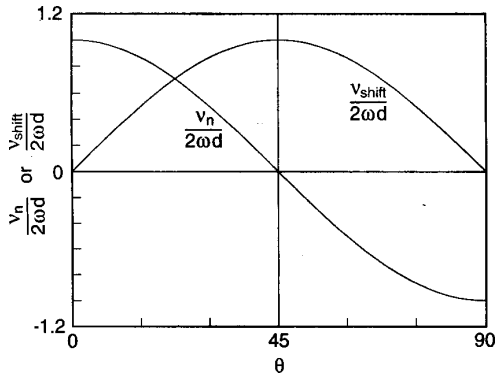

Fig. 8. Dimensionless normal velocity component and the velocity shift as functions of the mirror slope angle of θ for double reflection by two co-rotating mirrors

are taken at the mirror angles of 45° ± δ with δ ≈ 0, the corotating two-mirror system will effectively minimize the image biasing and maximize the velocity shift.

6 Concluding remarks

The systematic image errors have been identified from the normal displacement or the normal velocity component of PIV images occurring from a rotating mirror component. Detailed image kinematics have comprehensively described the two new ideas that are proposed to minimize the PIV systematic errors. Two linearly traversing mirrors, which substitute a single rotating mirror, can eliminate the systematic image errors and effectively generate the velocity shift. On the other hand, two co-rotating mirrors, instead of one, can reduce the systematic errors and maximize the velocity shift when the PIV images are taken at mirror slope angles close to 45°.

Appendix A: Derivation of the general expression for the reflected image velocity vector v_{image}

From substitution of Eq. (4) into Eq. (5), the general expression for the image velocity vector is derived as

$$\begin{aligned} \boldsymbol{v}_{\text{image}} &= \frac{d\boldsymbol{p}'}{dt} = \frac{d}{dt}\{[R]\cdot(\boldsymbol{p}-\boldsymbol{r}_m)+\boldsymbol{r}_m\} \\ &\frac{d[R]}{dt}\cdot(\boldsymbol{p}-\boldsymbol{r}_m)+[R]\cdot\frac{d}{dt}(\boldsymbol{p}-\boldsymbol{r}_m)+\frac{d\boldsymbol{r}_m}{dt} \\ &\frac{d[R]}{dt}\cdot(\boldsymbol{p}-\boldsymbol{r}_m)+[R]\cdot\boldsymbol{v}+(\boldsymbol{v}_m-[R]\cdot\boldsymbol{v}_m) \\ &\frac{d[R]}{dt}\cdot(\boldsymbol{p}-\boldsymbol{r}_m)+[R]\cdot\boldsymbol{v}+2(\boldsymbol{v}_m\cdot\boldsymbol{n})\boldsymbol{n} \end{aligned} \tag{A1}$$

where

$$\begin{aligned} \frac{d[R]}{dt}\boldsymbol{r} &= \frac{d}{dt}(\delta_{ij}-2n_in_j)r_j = \frac{d}{dt}(\delta_{ij}-2n_in_j)R_{jk}R_{kl}r_k \\ &-2(\Omega_in_j+n_i\Omega_j)R_{jk}r_k' \quad \text{with } \Omega_i = \frac{dn_i}{dt} \end{aligned} \tag{A2}$$

When the angular velocity of the rotating mirror is defined as ω, the amount of the mirror orientation change is given by Ω = ω × n. It is noted here that the component parallel to the normal vector does not contribute to the change of orientation. For Ω, ω and n is mutually perpendicular and n is a unit vector, ω = n × Ω, or equivalently, ($\omega_i = \varepsilon_{ijk}\, n_j\, \Omega_k$ is satisfied. Thus,

$$\varepsilon_{ilm}\omega_i = \varepsilon_{ilm}\varepsilon_{ijk}n_j\Omega_k = (\delta_{ij}\delta_{mk}-\delta_{ik}\delta_{mj})\,n_j\Omega_k = n_l\Omega_m-\Omega_ln_m \tag{A3}$$

$$\begin{aligned} (\Omega_in_j+n_i\Omega_j)R_{jk} &= (\Omega_in_j+n_i\Omega_j)(\delta_{jk}-2n_jn_k) \\ &= \Omega_in_k+n_j\Omega_k-2\Omega_in_k-n_i\Omega_k-\Omega_in_k \\ &= \varepsilon_{ijk}\omega_j = -\varepsilon_{jik}\omega_j \end{aligned} \tag{A4}$$

$$\frac{d[R]}{dt}\boldsymbol{r} = 2\varepsilon_{ijk}\omega_jr_k' = 2\boldsymbol{\omega}\times\boldsymbol{r}' \tag{A5}$$

where r' is identical to [R] · r as shown in Eq. (A2).

Substituting Eq. (A5) into Eq. (A1) gives the general expression for the image velocity vector of Eq. (6)

$$\boldsymbol{v}_{image} = 2\boldsymbol{\omega}\times\{[R]\cdot(\boldsymbol{p}-\boldsymbol{r}_m)\}+2(\boldsymbol{v}_m\cdot\boldsymbol{n})\boldsymbol{n}+[R]\cdot\boldsymbol{v} \tag{6}$$

Appendix B: Derivation of V;magez for the two co-rotating mirror system

The vector operator co x is expressed as

$$\boldsymbol{\omega}\times = \varepsilon_{ijk}\omega_j = \begin{bmatrix} 0 & -\omega & 0 \\ \omega & 0 & 0 \\ 0 & 0 & 0 \end{bmatrix} = \omega\begin{bmatrix} 0 & -1 & 0 \\ 1 & 0 & 0 \\ 0 & 0 & 0 \end{bmatrix} \tag{B1}$$

Then the first term of the final form of.Eq. (15) gives

$$\boldsymbol{\omega}\times([R]:[R]\cdot\boldsymbol{p}) = \omega\begin{bmatrix} 0 & -1 & 0 \\ 1 & 0 & 0 \\ 0 & 0 & 0 \end{bmatrix}\cdot\begin{bmatrix} \cos 2\theta & \sin 2\theta & 0 \\ \sin 2\theta & -\cos 2\theta & 0 \\ 0 & 0 & 1 \end{bmatrix}$$

$$\begin{bmatrix} \cos 2\theta & \sin 2\theta & 0 \\ \sin 2\theta & -\cos 2\theta & 0 \\ 0 & 0 & 1 \end{bmatrix}\begin{pmatrix} x \\ y \\ z \end{pmatrix},$$

$$= \omega\begin{bmatrix} 0 & -1 & 0 \\ 1 & 0 & 0 \\ 0 & 0 & 0 \end{bmatrix}\cdot\left(\begin{bmatrix} 1 & 0 & 0 \\ 0 & 1 & 0 \\ 0 & 0 & 1 \end{bmatrix}\cdot\begin{pmatrix} x \\ y \\ z \end{pmatrix}\right)$$

$$= \omega\begin{bmatrix} 0 & -1 & 0 \\ 1 & 0 & 0 \\ 0 & 0 & 0 \end{bmatrix}\cdot\begin{pmatrix} x \\ y \\ z \end{pmatrix} = \omega(-y, x, 0) \tag{B2}$$

The second term yields to

$$-\omega\times([R]\cdot\boldsymbol{r}_{m_2})=-\omega\begin{bmatrix}0&1&0\\1&0&0\\0&0&0\end{bmatrix}\left(\begin{bmatrix}\cos 2\theta&\sin 2\theta&0\\\sin 2\theta&-\cos 2\theta&0\\0&0&1\end{bmatrix}\cdot\begin{pmatrix}0\\-d\\0\end{pmatrix}\right)$$

$$=-\omega\begin{bmatrix}0&-1&0\\1&0&0\\0&0&0\end{bmatrix}\cdot\begin{pmatrix}-d\sin 2\theta\\d\cos 2\theta\\0\end{pmatrix}$$

$$=\omega d(\cos 2\theta,\sin 2\theta,0) \qquad \text{(B3)}$$

Substituting Eq. (14b) into the third term of Eq. (15) gives

$$[R]\cdot\boldsymbol{v}_{\text{image}_1}=\begin{bmatrix}\cos 2\theta&\sin 2\theta&0\\\sin 2\theta&-\cos 2\theta&0\\0&0&1\end{bmatrix}\cdot 2\omega\begin{pmatrix}-x\sin 2\theta+y\cos 2\theta\\x\cos 2\theta+y\sin 2\theta\\0\end{pmatrix}=2\omega(y,-x,0)$$

Substituting (B2), (B3), and (B4) into Eq. (15) gives

$$\boldsymbol{v}_{\text{image}_2}=2\boldsymbol{\omega}\times([R]:[R]\cdot\boldsymbol{p})-2\boldsymbol{\omega}\times([R]\cdot\boldsymbol{r}_{m_2})+[R]\cdot\boldsymbol{v}_{\text{image}_1}$$
$$=2\omega d(\cos 2\theta,\sin 2\theta,0) \qquad (16)$$

References

Adrian RJ (1986) Image shifting technique to resolve directional ambiguity in double-pulsed velocimetry. Appl Opt 25: 3855-3858

Keane RD; Adrian RJ (1992) Theory of cross-correlation analysis of PIV images. Appl Sci Res 49: 191-215

Merzkirch M; Mrosewski T; Wintrich H (1994) Digital particle image velocimetry applied to a natural convective flow. Acta Mechanica 4: 19-26

Oschwald M; Bechle S; Welke S (1995) Systematic errors in PIV by realizing velocity offsets with the rotating mirror method. Exp Fluids 18: 329-334

Prasad AK; Adrian RJ (1993) Stereoscopic particle image velocity applied to liquid flow. Exp Fluids 15: 49-60

Raffel M; Kompenhans J (1995) Theoretical and experimental aspects of image-shifting by means of a rotating mirror system for particle image velocimetry. Meas Sci Technol 6: 795-808